Biosensors and Bioelectronics 64 (2015) 449–455

Contents lists available at ScienceDirect

Biosensors and Bioelectronics

journal homepage: www.elsevier.com/locate/bios

Highly sensitive photoelectrochemical assay for DNA methyltransferase activity and inhibitor screening by exciton energy transfer coupled with enzyme cleavage biosensing strategy

Qingming Shen [a,*], Li Han [a,b], Gaochao Fan [b], E.S. Abdel-Halim [c], Liping Jiang [b,*], Jun-Jie Zhu [b]

[a] Key Lab of Organic Electronics & Information Displays, Institute of Advanced Materials, Nanjing University of Posts and Telecommunications, Nanjing 210023, PR China
[b] State Key Laboratory of Analytical Chemistry for Life Science, School of Chemistry and Chemical Engineering, Nanjing University, Nanjing 210093, PR China
[c] Petrochemical Research Chair, Department of Chemistry, College of Science, King Saud University, P.O. Box 2455, Riyadh 11451, Kingdom of Saudi Arabia

ARTICLE INFO

Article history:
Received 23 July 2014
Received in revised form
15 September 2014
Accepted 19 September 2014
Available online 28 September 2014

Keywords:
DNA methylation
Methyltransferase
Photoelectrochemistry
Exciton energy transfer
Enzyme cleavage

ABSTRACT

Highly sensitive DNA methyltransferase (MTase) activity and inhibitor screening photoelectrochemical (PEC) assay was developed based on the exciton energy transfer (EET) effect coupled with site-specific cleavage of restriction endonuclease (HpaII). The assay was designed by integrating the Au nanoparticles (NPs) labeled probe DNA (pDNA-Au) with CdSe quantum dots (QDs). The strong EET effect between Au NPs and CdSe QDs resulted in the dramatic decrease of photocurrent signal. The pDNA carried a sensing region for specifically recognizing target DNA (tDNA) and hybridizing with it to form a DNA duplex. With the site-specific cleavage of HpaII, the DNA duplex could be cleaved and Au NPs would be released, which broke the EET and resulted in the restoration of photocurrent signal. However, when the DNA duplex was methylated by M.SssI MTase, this cleavage of HpaII was blocked, and therefore the unbroken EET effect kept the lower photocurrent signal. That was, the restored photocurrent was inversely proportional to the MTase activity. Based on this strategy, the PEC assay could determine as low as ~0.0042 U/mL of M. SssI MTase with a linear range from 0.01 to 150 U/mL. In addition, the assay could be used for the screening of the inhibitors of MTase. This PEC assay provides a promising platform for monitoring the activity and inhibition of DNA MTase, and thus shows a great potential in cancer diagnostics and anti-cancer drugs discovery.

1. Introduction

As one of the most important epigenetic events, DNA methylation plays a crucial role in numerous biological systems, including cell proliferation, gene transcription, and senescence (Reik et al., 2001). Aberrant DNA methylation always associates with canceration because it can inactivate the tumor suppressor genes and lead to transcriptional silencing of gene expression (Baylln et al., 1997; Kass et al., 1997). The overexpression of methylated DNA has been found in many cancers, such as thyroid tumors and human breast cancers, and so on (Miyamoto et al., 2005). DNA methylation process is catalyzed by DNA methyltransferases (MTase), which can recognize specific DNA sequences and transfer a methyl group from the cofactor S-adenosyl-L-methionine (SAM) to the C-5/N-4 of cytosine and the N-6 of adenine residues (Adams, 1990; Grandjean et al., 2007; Song et al., 2009). Therefore, the activity of MTase will affirmatively influence the DNA methylation level. On the other hand, the DNA MTase has also been treated as predictive biomarkers and potential therapeutic targets for cancers diagnosis and anticancer drugs in clinic (Heithoff et al., 1999; Low et al., 2001). Therefore, the development of simple and sensitive methods for identification and quantification of the DNA methylation level and DNA MTase activity assay is highly desirable in basic biomedical research and may provide an applicable approach for the early diagnosis of the related cancers and anti-cancer drug discovery. Up to now, various methods have been developed for the determination of DNA methylation and assay of MTase activity, such as polymerase chain reaction-based (PCR) technique (Hatada et al., 1991; Lyko et al., 2000), surface enhanced Raman spectroscopy (SERS) (Hu and Zhang, 2011), capillary electrophoresis (Fraga et al., 2000, Wang et al., 2009b), gel electrophoresis (McLaughlin et al.,1987), electrochemistry (Liu et al., 2011; Tsutsui et al., 2011), high-performance liquid chromatography (HPLC) (Friso et al., 2002), colorimetric methods (Liu et al., 2009; Wu et al., 2013), fluorescence method (Bi et al., 2013; Li et al.,

* Corresponding authors. Fax: +86 25 85866396.
E-mail addresses: iamqmshen@njupt.edu.cn (Q. Shen), jianglp@nju.edu.cn (L. Jiang).

http://dx.doi.org/10.1016/j.bios.2014.09.044
0956-5663/

2007; Wang et al., 2013; Zhao et al. 2013), light scattering (Zhao et al., 2011a), photoelectrochemical method (PEC) (Zhou et al., 2014) and electrogenerated chemiluminescence (ECL) method (Kurita et al., 2012; Li et al., 2012; Li et al., 2013), etc.

Among them, PEC methods have attracted more attention because of the advantages of cheap instruments, simple operation and high sensitivity and selectivity. Its sensing principle bases on the corresponding photocurrent signals change originated from the biorecognition or biocatalytic events. Coupling photoirradiation with an electrochemical system, PEC possesses the advantages of high selectivity and sensitivity because of the separation forms of excitation source (light) and detection signal (electric current). In addition, the use of electronic readout makes the instrument simpler, cheaper, and easier to miniaturize than that of optical methods. However, the signaling mechanism of current PEC assay is mainly limited to altering electron donor concentration or changing the diffusion efficiency by affinity reaction to achieve the signal diminution/enhancement (Chen et al., 2010; Fan et al., 2014; Kang, et al., 2011; Wang et al., 2010; Yildiz et al., 2008; Zhang et al., 2010; Zhao et al., 2012b; Zhu et al., 2009). That is, the signaling strategy was mostly established on the interfacial electron transfer between the photoactive material and ambient environment (Gill et al., 2008). Hence, it would be desirable to find a more sensitive and effective method for photocurrent signaling system.

Recently, the Förster resonance energy transfer between semiconductor nanocrystals and metallic nanoparticles has been demonstrated as an advanced and feasible energy transfer based bioassay protocol (Govorov et al., 2006; Lee et al., 2007; Shan et al., 2009; Wang et al., 2011; Zhang et al., 2014). The exciton energy transfer (EET) from the CdSe quantum dots (QDs) to the Au NPs in PEC system was also investigated by using the spontaneous emission originated from the radioactive decay of the former to activate the latter (Zhao et al., 2012a).

In this paper, a novel, sensitive PEC assay for DNA MTase activity was developed based on the EET between CdSe QDs and Au NPs coupled with site-specific cleavage of restriction endonuclease biosensing strategy. Due to the inherent overlaps between exciton band of CdSe QDs with the plasmon band of Au NPs, the strong EET between them could diminish the photocurrent signal of the CdSe QDs (Scheme 1). As shown in Scheme 2, to fabricate EET-based PEC biosensor, the TiO_2 film and CdSe QDs were modified on an indium tin oxide (ITO) electrode, respectively. Then, the Au NPs labeled probe DNA (pDNA-Au) was immobilized on the ITO/TiO_2/CdSe electrode by coupling reaction between –COOH of CdSe and $–NH_2$ of pDNA-Au. The bound pDNA-Au could induce an obvious decrease of photocurrent signal by the strong EET effect between CdSe QDs and Au NPs. The selective detection mechanism based on the site-specificity of HpaII endonucleases cleavage of the 5′-CCGG-3′ DNA sequence (Duan et al., 2013). The DNA duplex could be digested by the HpaII endonucleases, resulting in the recovery of photocurrent intensity of the assay. After methylation by M.SssI MTase, the 5′-CCGG-3′ DNA sequence could be recognized and catalyzed by M.SssI MTase and transfer a methyl group from S-adenosyl-methionine (SAM). Since the methylated DNA could not be digested by the HpaII endonucleases, the unbroken EET kept the lower photocurrent signal. The more activity the M.SssI MTase had, the more DNA was methylated, the more EET was maintained, and subsequent the lower photocurrent signal was restored. Namely, the restored photocurrent was inversely proportional to the DNA methylation level and the activity of M.SssI MTase. Therefore, the PEC assay for DNA MTase activity was developed by EET between CdSe QDs and Au NPs coupled with enzyme cleavage biosensing strategy successfully. Furthermore, the application of the proposed sensing strategy for screening MTase inhibitors was also demonstrated with satisfactory results. This novel method not only provides a promising platform for monitoring activity and inhibition of DNA MTases, but also shows great potentials in cancer diagnostics and anti-cancer drugs discovery.

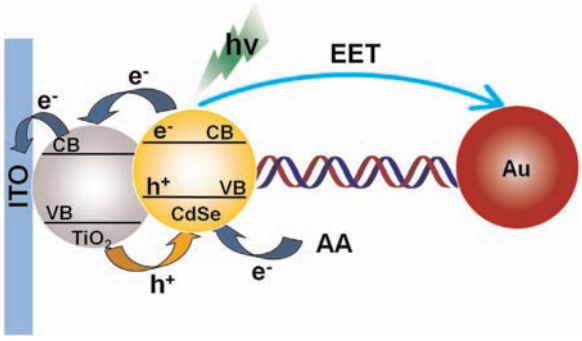

Scheme 1. Energy transfer between CdSe QDs and Au NPs.

2. Experimental

2.1. Materials and reagents

TiO_2 powder was purchased from the Degussa Co. (P25, Germany). Cadmium chloride ($CdCl_2 \cdot 2.5H_2O$) and chloroauric acid ($HAuCl_4 \cdot 4H_2O$) were obtained from Shanghai Chemical Reagent Co. (China). Hydrochloric acid (HCl), sodium chloride (NaCl), sodium hydroxide (NaOH) and magnesium chloride hexahydrate ($MgCl_2 \cdot 6H_2O$) were obtained from Nanjing Chemical Reagent Co. Ltd. (China). Tris (hydroxymethyl) aminomethane (Tris) and ascorbic acid (AA) were purchased from Sinopharm Chemical Reagent Co. Ltd. (China). Selenium powder (Se), 1-ethyl-3-(3-dimethylaminopropyl) carbodiimide (EDC), N-hydroxysuccinimide (NHS), sodium borohydride ($NaBH_4$), thioglycolic acid (TGA), bovine serum albumin (BSA), tris (2-carboxyethyl) phosphine hydrochloride (TCEP, 98%), catechol-O-methyltransferase (COMT), polydimethyl diallyl ammonium chloride (PPDA), fisetin and 5-flurouracil were received from Sigma-Aldrich (USA). S-adenosyl-methionine (SAM), CpG methyltransferase (M.SssI MTase), 10 × NEBuffer 2, HpaII endonuclease and 1 × CutSmart Buffer were obtained from New England BioLabs (Ipswich, MA). All aqueous solutions were prepared and diluted using ultrapure water (18.2 MΩ/cm) obtained from the Millipore Milli-Q system.

The synthetic DNA was purchased from Sangon Biotechnology Co. Ltd. (Shanghai, China) with base sequences are as follows:

pDNA (S1): 5′-NH_2-$(CH_2)_6$-GCT CCG GAT CTC CCT TCC CAG GAC GC-$(CH_2)_6$-HS-3′;

tDNA (S2): 5′-GCG TCC TGG GAA GGG AGA TCC GGA GC-3′;

One-based mismatch (S3): 5′- GCG TCA TGG GAA GGG AGA TCC GGA GC-3′;

Two-based mismatch (S4): 5′- GCG TCC TGC GAT GGG AGA TCC TGA GC-3′;

Noncomplementary DNA (S5): 5′-CTC GCT AAT AAC AAT GAT CAC AGC TA-3′.

The synthesized oligonucleotides were dissolved in 10 mM tris-HCl (pH = 7.4, M_{NaCl} = 0.1 M) to desired stock concentrations and stored at –20 °C according to the manufacturer's instructions.

The buffer solutions employed in this study are as follows. Probe immobilization buffer: 10 mM Tris–HCl, 0.1 M NaCl (pH 7.4). DNA hybridization buffer: 10 mM Tris–HCl, 0.1 M NaCl and 20 mM $MgCl_2$ (pH 7.4). 1 × NEBuffer 2: 50 mM NaCl, 10 mM Tris–HCl, 10 mM $MgCl_2$, 1 mM dithiothreitol (pH 7.9). 1 × CutSmart Buffer: 50 mM KAc, 20 mM Tris–Ac, 10 mM $Mg(Ac)_2$, 100 μg/ml BSA, pH = 7.9. Photoelectrochemical determination buffer: 0.1 M PBS

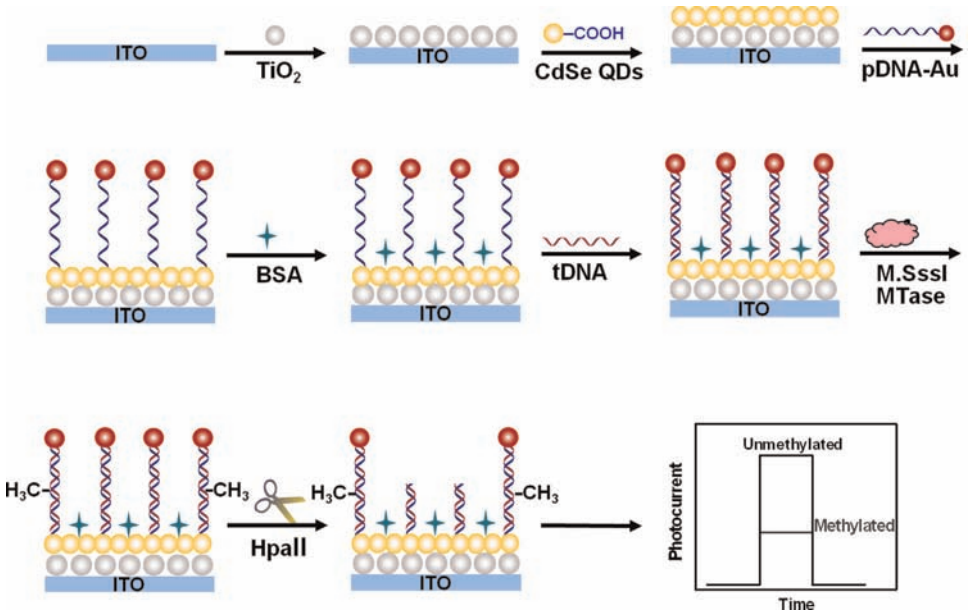

Scheme 2. Schematic illustration of PEC assay for DNA MTase activity fabricated by using EET between CdSe QDs and Au NPs coupled with site-specific cleavage of restriction endonuclease biosensing strategy.

(pH 7.4) was prepared by mixing the stock solution of 0.1 M NaH_2PO_4 and 0.1 M Na_2HPO_4, and the pH was adjusted by NaOH or HCl. All reagents were analytically pure grade.

2.2. Apparatus

The morphology and particle size of the samples were characterized by high resolution transmission electron microscope (HRTEM) (JEOL-2100, Japan). The UV-visible (UV–vis) absorption spectra were obtained on a UV-3600 UV–vis spectrophotometer (Shimadzu, Japan). Photoluminescence (PL) spectra were obtained on an RF-5301PC spectrophotometer (Shimadzu). Electrochemical impedance spectroscopy (EIS) was performed on an Autolab potentiostat/galvanostat (PGSTAT 30, Eco Chemie B.V., Utrecht, Netherlands) with a three-electrode system in 0.1 M KCl solution containing 5.0 mM $K_3[Fe(CN)_6]/K_4[Fe(CN)_6]$ (1:1) mixture as a redox probe, and recorded in the frequency range of 0.01 Hz–100 kHz with an amplitude of 50 mV. Photoelectrochemical measurements were carried out with a homemade photoelectrochemical system. A 500 W Xe lamp was used as the irradiation source with the light intensity of 400 μW cm^{-2} estimated by a radiometer (Photoelectric Instrument Factory of Beijing Normal University). Photocurrent was recorded on a CHI 660D electrochemical workstation (Shanghai Chenhua Apparatus Corporation, China), and ITO modified electrode, saturated calomel electrode (SCE) electrode, platinum wire were used as working, reference, and counter electrode in this work, respectively. All photocurrent measurements were carried out in PBS (pH 7.4, 0.1 M) containing 0.1 M AA (an efficient electron donor employed in this work) at room temperature with 0 V applied potential. The AA electrolyte was deaerated by pumping into nitrogen for 10 min before photoelectrochemical experiments.

2.3. Preparation of CdSe QDs

Water soluble CdSe QDs were synthesized according to the literature by using thiolglycolic acid as the capping agent (Jiang and Ju, 2007). Briefly, NaHSe aqueous solution was prepared by dissolving Se powder in $NaBH_4$ solution under nitrogen atmosphere at room temperature. After 50 mL of 2 mM $CdCl_2$ solution was mixed with 20 μL of TGA (pH = 10) and bubbled with highly pure N_2 for 30 min, 0.7 mL of 70 mM NaHSe precursors solution was added in the mixture to obtain a clear, lightly yellow solution. The optimum molar ratios of Cd^{2+}/Se^{2-}/TGA for the preparation of CdSe QDs were 1:0.5:2.5. The obtained solution was then refluxed at 100 °C for 4 h to form TGA-modified CdSe QDs.

2.4. Synthesis of Au NPs

Au NPs with average diameter 5 ± 1 nm were prepared according to the previous report (Zhao et al., 2011b). All glassware used in the synthetic process were immersed in freshly prepared aqua regia (HNO_3/HCl = 1:3) for 10 h, then washed cleanly with ultrapure water, and dried at 80 °C. Briefly, 0.6 mL of 0.1 M ice cold $NaBH_4$ solution was added to 20 ml 250 μM $HAuCl_4$ aqueous solution under stirring. The solution immediately turned to an orange-red color, indicating the formation of Au NPs. And then the solution was kept stirring in an ice bath for 10 min. Finally, the solution reacted at room temperature for another 3 h with the color changing from orange-red to wine red. The prepared monodisperse Au NPs were stored at 4 °C for further use.

2.5. Functionalization of Au NPs with thiolated DNA

First, 20 μL of pDNA (50 μM) solution activated by 10 μL TCEP (10 mM) for 1 h (Burns et al., 1991; Zhang et al., 2007), then, 800 μL freshly prepared colloid Au NPs was added into above solution. In order to assure the fastness of Au-S bond, the mixture was shaken gently for 16 h at room temperature. Then the mixed solution was centrifugated for 30 min at 15000 rpm. Finally, the red precipitate was redispersed in 10 mM Tris–HCl containing 0.1 M NaCl (pH 7.4). The pDNA-Au solution was reserved at 4 °C before use.

2.6. Fabrication of PEC biosensor

The ITO slices were used as the working electrodes, which were washed by immersing in ethanol/NaOH mixed solution (v/v, 1:1), acetone and double distilled deionized water, respectively, followed drying at 60 °C for 2 h. Then, 20 μL of TiO_2 dispersion

(1 mg/mL) was dropped onto a piece of ITO slice with fixed area of 0.25 cm^2. After drying in air, the obtained ITO/ TiO_2 electrodes were calcined at 450 °C for 30 min and finally cooled down to room temperature. To study the influence of the thickness of TiO_2 to the photocurrent, different concentrations of TiO_2 solution (0.5, 0.75, 1.0, 1.25, 1.5 and 2.0 mg/mL) were dropped on the ITO slices. Subsequently, the ITO/TiO_2/CdSe modified electrode was fabricated via layer by layer assembling (Wang et al., 2009a), it was performed by alternatively dipping ITO/TiO_2 electrode in 1% PDDA and CdSe QDs solution (10 min each) with intermediate distilled water washings until desired number of bilayers were assembled onto the ITO/TiO_2 substrate.

After that, the ITO/TiO_2/CdSe modified electrodes were immersed in a solution containing 10 mM EDC and 20 mM NHS for 30 min at room temperature. Then, 20 μL pDNA-Au suspension (1 μM) was casted onto ITO/TiO_2/CdSe electrode surface for 12 h under humid conditions, followed by washing with 10 mM Tris–HCl (pH 7.4) for three times, and pDNA-Au was conjugated onto as-prepared electrode by EDC–NHS coupling reactions between –COOH groups on the surface of CdSe QDs and the $-NH_2$ groups of pDNA. After blocking with 1% BSA solution, the modified electrode was dipped into 20 μL tDNA (1 μM) and incubated at 37 °C for 2 h under humid conditions, followed by rinsing with 10 mM Tris–HCl (pH 7.4) for three times.

The electrode was further incubated in the stock buffer containing 160 μM SAM and different concentration of M.SssI MTase at 37 °C for 2 h under humid conditions, followed by rinsed with 10 mM Tris–HCl (pH 7.4) for three times. Finally, the hybridized DNA cleaved by HpaII endonucleases was performed at 37 °C for 2 h by dropping 20 μL 1 × CutSmart Buffer containing 40 U/mL HpaII on the electrode surface at humid condition. After cleavage, the electrode was rinsed with 10 mM Tris–HCl (pH 7.0) and dried with nitrogen.

3. Results and discussion

3.1. Characterization of Au NPs and CdSe QDs

To confirm the successful synthesis of CdSe QDs and Au NPs, HRTEM was performed. As shown in Fig. 1A, the size of the CdSe QDs was about 3 nm. Fig. 1B is the typical HRTEM image of Au NPs, showing that the diameter of Au NPs was about 5 nm with a uniform size distribution. For the efficient EET, the spectra overlap between the emission spectra of the CdSe QDs and absorption spectra of Au NPs is essential. As can be seen in Fig. 1C, a dominant absorption peak at 512 nm, arousing by the surface plasmon resonance (SPR) of Au NPs could be clearly observed. The peak of CdSe QDs PL spectrum was at 554 nm. Evidently, the PL emission of the CdSe QDs had a considerable spectral overlap with the absorption of the Au NPs, which would be beneficial to the inducement of the SPR of the Au NPs and thus affected the subsequent interparticle energy transfer, leading to the reduction of the photocurrent (Wang et al., 2011; Zhao et al., 2011b).

3.2. EIS of the biosensor

It is well known that EIS could provide important information on the features of modified electrode surfaces. Normally, the EIS includes a semicircle portion and a linear portion. The semicircle portion at higher frequencies represents the electron transfer limited process, and the linear portion at lower frequencies is due to the diffusion limited process. The semicircle diameter equals the electron-transfer resistance (R_{et}), which reflects the electron-transfer kinetics of the redox probe at the electrode interface. At present, to a large extent, R_{et} proves the restricted diffusion of the redox probe through the multilayer system, and proves directly the film permeability (Lu and Hu, 2006; Wang et al., 2004). Fig. 2A shows the Nyquist plots of impedance spectrum corresponding to the different stages and the inset shows the applied equivalent circuit. The bare ITO electrode displayed a near-straight line (curve a), implying a very small electron transfer resistance, which meant that $[Fe(CN)_6]^{4-/3-}$ could reach the electrode surface and exchange charge readily. After the deposition of TiO_2 layer (curve b), the semicircle diameter did not change much, which implied that the R_{et} changed little. When the electrode modified with PDDA/CdSe (curve c), the R_{et} increased obviously on account of the hindrance effect of PDDA/CdSe. However, the R_{et} decreased when the pDNA-Au was assembled onto the electrode (curve d). It could be attributed to the good conductivity of Au NPs, which could accelerate the electron transfer (Zhou, et al., 2014). Subsequently, when BSA was immobilized on the electrode (curve e), the R_{et} increased obviously because the nonconductive proteins obstructed electron transfer severely and prevented the redox probe reaching the electrode surface. After the as-prepared biosensor was incubated with the corresponding target DNA, the R_{et} increased further (curve f), which was ascribed to the increase of steric hindrance effect. Finally, when the electrode was incubated in the buffer containing HpaII (curve g), the R_{et} decreased, indicating the successful digestion of DNA.

3.3. Photoelectrochemical characterization of biosensor

The fabrication process of PEC biosensor was also characterized by monitoring the photocurrent in 0.1 M PBS (pH 7.4) containing 0.1 M AA as electron donor. As illustrated in Fig. 2B, the ITO/TiO_2 electrode shows a proper photocurrent (curve a), because TiO_2 can only absorb ultraviolet light, resulting in low photo-to-current conversion efficiency. After the CdSe QDs deposited, as

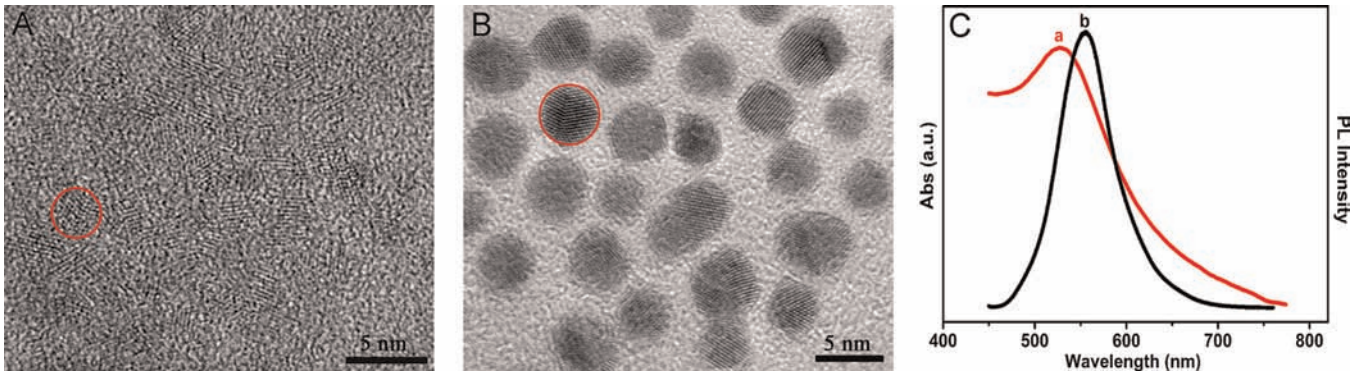

Fig. 1. HRTEM images of (A) CdSe QDs; (B) Au NPs; (C) Absorption spectrum of (a) Au NPs and (b) the corresponding PL spectra of pure CdSe QDs.

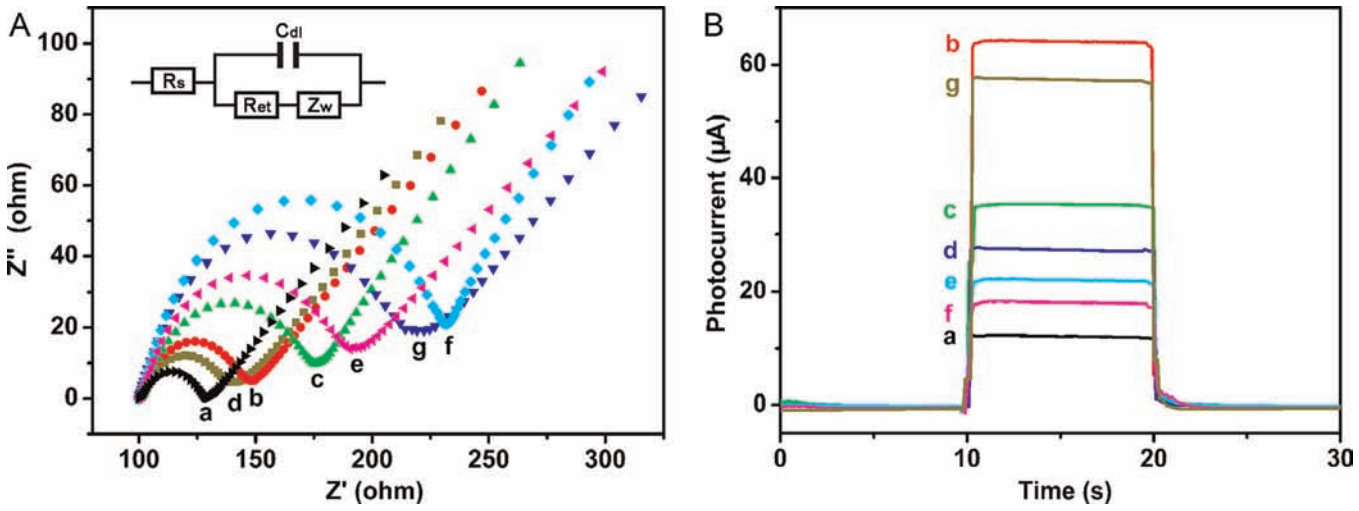

Fig. 2. (A) Nyquist plot of different modified electrodes in 0.1 M KCl solution containing 5.0 mM $K_3Fe(CN)_6/K_4Fe(CN)_6$ (1:1): (a) bare ITO; (b) TiO_2; (c) TiO_2/CdSe; (d) TiO_2/CdSe/pDNA-Au; (e) TiO_2/CdSe/pDNA-Au/BSA; (f) TiO_2/CdSe/pDNA-Au/BSA/tDNA (1×10^{-6} M); (g) TiO_2/CdSe/pDNA-Au/BSA/tDNA (1×10^{-6} M)/HpaII (40 U/ml). The inset is the equivalent circuit. R_s, R_{et}, Z_w and C_{dl} represent ohmic resistance of the electrolyte, electron transfer resistance, Warburg impedance and the double-layer capacitance, respectively; (B) photocurrent response of the modified different ITO electrode in 0.1 M PBS (pH 7.4) containing 0.1 M ascorbic acid: (a) TiO_2; (b) TiO_2/CdSe; (c) TiO_2/CdSe/pDNA-Au; (d) TiO_2/CdSe/pDNA-Au/BSA; (e) TiO_2/CdSe/pDNA-Au/BSA/tDNA (1×10^{-6} M); (f) TiO_2/CdSe/pDNA-Au/BSA/tDNA (1×10^{-6} M)/M.SssI MTase (160 μM SAM, 260 U/ml MTase)/HpaII (40 U/mL); (g) TiO_2/CdSe/pDNA-Au/BSA/tDNA (1×10^{-6} M)/HpaII (40 U/mL).

demonstrated in curve (b), the photocurrent increased obviously, which was due to the sensitization effect of CdSe QDs. The introduction of narrow band gap CdSe QDs as the photosensitizer to large band gap TiO_2 was favorable for the generation and separation of electron–hole pairs under visible light, leading to the enhanced photocurrent intensity (Santz and Kamat, 2002; Tambwekar et al., 1999; Borgarello et al., 1985). Subsequently, when pDNA-Au was bound on the electrode (curve c), the photocurrent signal substantially diminished on account of the EET between CdSe QDs and Au NPs. After BSA and tDNA immobilized on the modified electrode successively (curve d and e), the photocurrent decreased gradually. This could be attributed to the fact that the immobilization of BSA and tDNA on the ITO/TiO_2/CdSe/pDNA-Au electrode increased the steric hindrance effect, which partly obstructed the electron donor-AA to the surface of CdSe QDs and scavenged the photogenerated holes. When the electrode was incubated with M. SssI MTase and HpaII endonucleases successively (curve f), the photocurrent with little change should be ascribed to superfluous mount M.SssI MTase, indicating that all DNA were methylated, thus, no DNA could be digested. However, the control experiments showed significant photocurrent recovery of TiO_2/CdSe/pDNA-Au/BSA/tDNA/HpaII modified ITO electrode (curve g), because the HpaII endonucleases digestion of the unmethylated DNA, and thus cut off the EET effect between CdSe QDs and Au NPs.

3.4. Optimization of experimental conditions

In order to observe the optimal concentration of TiO_2, we prepared different concentration of TiO_2 solution with the fixed coating number of CdSe QDs. As shown in Fig. S1A, the figure indicated that when the TiO_2 solution was 1 mg/ml, the photocurrent intensity was the strongest. With the increase of the concentration of the TiO_2 solution, TiO_2 film was thicker, suggesting that the electrode had more surface area and absorb more PDDA/CdSe QDs (Park et al., 2000). However, further increased the thickness of TiO_2 film could augment the charge diffusion resistance with more surface recombination centers on excessive TiO_2 film, and lead to the decrease of photocurrent. (Kuang et al., 2006). Thus, 1.0 mg/mL TiO_2 solution was selected as the optimal concentration.

It is well known that photocurrent intensity will be desirable for applications of QDs in biosensing, which could increase the signal/noise ratio (S/N). The numbers of the alternating PDDA/CdSe QDs composite multilayer films were monitored by photocurrent measurement. Fig. S1B showed the photocurrent of $(PDDA/CdSe)_n$ films with TiO_2 film for identical concentration. The results demonstrated that when the coating layer number of PDDA/CdSe QDs was five, the photocurrent was the highest, indicating that the surface of TiO_2 was covered with PDDA/CdSe QDs completely. When CdSe QDs were superfluous, the charge diffusion resistance increased and more surface recombination centers subsequently, leading to the reduced photocurrent (Vogel et al., 1994).

The optimal methylation time of MTase played a significant role for optimizing the photocurrent signal. As shown in Fig. S1C, it was estimated by the photocurrent with different methylation time. The data demonstrated that the longer methylation time, the lower of the photocurrent. The reason was that with the longer methylation time, the more double DNA was methylated, the fewer double DNA could be cleaved, resulting in the lower photocurrent. Therefore, we selected 120 min as the optimal methylation time.

3.5. Calibration curve of the PEC biosensor

The photocurrent response for the modified electrode was found to be related to the concentration of the M.SssI MTase. Thus, photocurrent intensity was used to analyze the DNA methylation and activity of M.SssI MTase. As shown in Fig. 3A, the photocurrent response altered according to the different concentration of M.SssI MTase. The Fig. 3B showed a broad linear relationship between the photocurrent and the logarithm of concentration of MTase in the range of 0.01–150 U/mL with a correlation coefficient (R) of 0.998, and the linear fitting equation is

$$I = 36.20 - 6.34 \lg[c],$$

where I is the photocurrent, c is the concentration of M.SssI MTase. The detection limit could be calculated as 0.0042 U mL^{-1} based on the 3σ rule ($S/N=3$), which was much lower than the previous reports (as shown in Table 1), indicating that this method was an

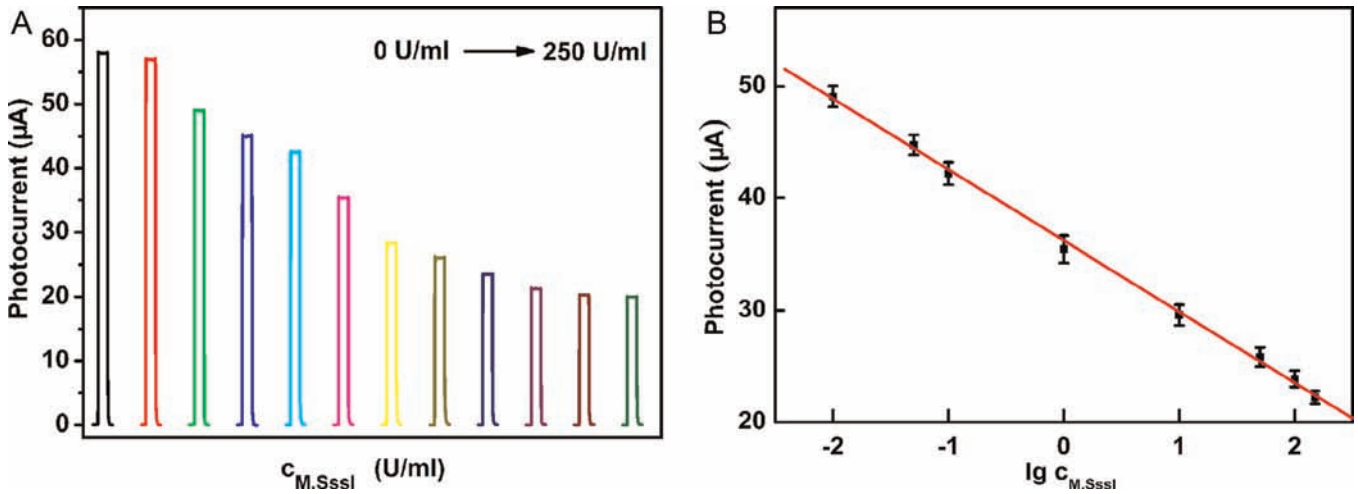

Fig. 3. (A) Photocurrent response of the PEC assay treated with different concentration of M.SssI MTase. The concentrations of M. SssI MTase were 0, 0.005, 0.01, 0.05, 0.1, 1, 10, 50, 100, 150, 200 and 250 U/mL, respectively. (HpaII was 40 U/mL) (B) The linear calibration curve of the different concentration of M.SssI MTase. Error bars represent standard deviations of measurements (n=5).

Table 1
Analytic performance of diverse methods to detect the M.SssI MTase activity.

Method	Linear range (U/mL)	Detection limit (U/mL)	Reference
Light scattering assay	10–100	10	Zhao et al. (2011a)
Colorimetric biosensor	0–64	0.7	Wu et al. (2013)
Chemical luminescene	1–10	0.52	Bi et al. (2013)
Electrochemical strategy	0.25–10	0.18	Wang et al. (2013)
Bioluminescence assay	0.2–2.5	0.08	Jiang et al. (2012)
Fluorescene assay	0.1–4	0.06	Zhao et al. (2013)
Electrochemiluminescence	0.05–100	0.02	Li et al. (2012)
PEC	0.1–50	0.035	Zhou et al. (2014)
PEC	0.01–150	0.0042	This work

effective way to detect DNA methylation and assay activity of M. SssI MTase.

3.6. Selectivity, reproducibility and stability of the PEC biosensor

To further verify the selectivity of the proposed PEC biosensor for the tDNA. The prepared TiO_2/CdSe/pDNA-Au/BSA electrobe was incubated in the buffer containing tDNA with a mismatch of different amount of base. As seen in Fig. S2, it was clear that remarkable changes of photocurrent signals were observed as compared to the tDNA with no mismatched base. On the other hand, weaker photocurrent signals were found by replacing with base-mismatched tDNA. The fact demonstrated that the as-proposed PEC biosensor had an excellent selectivity. The present method operates via detecting the recovered photoelectrochemical signal, which is a combined result of the specific methylation and the site-specific endonuclease cleavage; thus, the assay should be relatively impervious to false signals arising due to the non-specific adsorption of interferents.

The reproducibility of the proposed PEC biosensor was assessed through the analysis of five independently prepared biosensors. The photocurrent signal gave a relative standard deviation (RSD) with intraassay and interassay precision. The intraassay precision was obtained by measuring M.SssI MTase with the concentration of 0.1 U/mL five times, which gave a RSD of 3.2%. The interassay precision was gained by assaying the M.SssI MTase with the same concentration for 10 electrodes, the RSD was 3.6%. According to the above data, the as-proposed PEC biosensor showed a good reproducibility.

The stable photocurrent response of the PEC assay treated with 10 U/mL M.SssI MTase indicated the good stability (Fig. S4). The stability of the biosensor was also estimated from the change of photocurrent signal for the electrode with different storage time. The PEC biosensors were stored in the PBS (pH 7.4) solution at 4 °C for a week and a month respectively. The photocurrent response retained 96.3% and 90.8% value of the initial response respectively, which showed a quite satisfying stability.

3.7. Inhibition of M.SssI MTase activity

To further study the potential application of this biosensor in screening of MTase inhibitor, the inhibition experiment was performed in the presence of two model inhibitor, fisetin and 5-fluorouracil, respectively. These compounds are representative anticancer drugs used in a large number of clinical trials and in the majority of methylation inhibition experiments (Khan, et al., 2008; Gamelin and Boisdron-Celle, 1999). The relative activity (%) is estimated as follows:

$$\text{RA (relative activity)} = (I_0 - I_i)/(I_0 - I_t) \times 100\%$$

where I_0, I_t, and I_i were the photocurrent signal in the absence of M.SssI MTase, in the presence of M.SssI MTase, and in the presence of both M.SssI MTase and different concentration of inhibitor, respectively. As shown in Fig. S3, with the increasing of inhibitor concentration, the RA of the MTase gradually dropped. The 5-fluorouracil and fisetin were found to inhibit 50% M.SssI MTase activity (The IC_{50} value, the inhibitor concentration required to reduce the enzyme activity by 50%) with 1.0 μM and 80.0 μM, respectively. Thus, in comparison with fisetin, the 5-fluorouracil revealed much stronger inhibition efficiency to M.SssI MTase activity in the same concentration, which was in good agreement with previous MTase activity assay (Yin, et al., 2013; Zhou, et al., 2014). This result also showed that the PEC biosensor has the potential ability to screen the inhibitors to DNA MTase.

4. Conclusion

In summary, we have described a highly sensitive PEC assay for MTase activity and inhibitor screening. The present method was

based on EET effect coupled with the site-specific endonuclease cleavage. The intensity of the restored photocurrent signal was inversely proportional to the MTase activity. Based on the strategy, the PEC assay could determine as low as ~0.0042 U/mL of M.SssI MTase with a linear range from 0.01 to 150 U/mL. The assay showed relatively impervious to false signals arising due to the nonspecific adsorption of interferents. Moreover, the assay could be also used for screening of the inhibitors of MTase, which might be help for the discovery of anticancer drugs. The developed PEC assay can be expected to be an attractive candidate for sensitive MTase activity monitoring, and supply valuable information for biomedical research, early clinical diagnosis and anti-cancer drugs discovery.

Acknowledgements

We are grateful to the financial support of National Natural Science Foundation of China (21105050, 21475057), Program for New Century Excellent Talents in University (NCET-12-0256), Ministry of Education of the People's Republic of China (No. IRT1148), Research Found for the Doctoral Program of Higher Education of China (20113223120004), the Foundation of the Jiangsu Education Committee (14KJB150015), Synergetic Innovation Center for Organic Electronics and Information Displays and a Project Funded by the Priority Academic Program Development of the Jiangsu Higher Education Institutions. The Authors extend their appreciation to the Deanship of Scientific Research at King Saud University for funding the work through the Research Group Project (RGP-VPP-029).

Appendix A. Supplementary Information

Supplementary data associated with this article can be found in the online version at http://dx.doi.org/10.1016/j.bios.2014.09.044.

References

Adams, R.L.P., 1990. Biochem. J. 265, 309–320.
Baylln, S.B., Herman, J.G., Graff, J.R., Vertino, P.M., Issa, J.P., George, F.V.W., George, K., 1997. Adv. Cancer Res. 72, 141–196.
Bi, S., Zhao, T.T., Luo, B.Y., Zhu, J.J., 2013. Chem. Commun. 49, 6906–6908.
Borgarello, E., Harris, R., Serpone, N., 1985. New J. Chem. 9, 743–747.
Burns, J.A., Butler, J.C., Moran, J., Whitesides, G.M., 1991. J. Org. Chem. 56, 2648–2650.
Chen, D., Zhang, H., Li, X., Li, J.H., 2010. Anal. Chem. 82, 2253–2261.
Duan, A.P., Ning, L.M., Li, C., Hou, Y.F., Yang, N.N., Sun, L.Z., Li, G.X., 2013. Sci. China Life Sci. 56, 293–297.
Fan, G.C., Ren, X.L., Zhu, C., Zhang, J.R., Zhu, J.J., 2014. Biosens. Bioelectron 59, 45–53.
Fraga, M.F., Rodriguez, R., Canal, M.J., 2000. Electrophoresis 21, 2990–2994.
Friso, S., Choi, S.W., Dolnikowski, G.G., Selhub, J., 2002. Anal. Chem 74, 4526–4531.
Gamelin, E., Boisdron-Celle, M., 1999. Crit. Rev. Oncol. Hematol. 30, 71–79.
Gill, R., Zayats, M., Willner, I., 2008. Angew. Chem. Int. Ed. 47, 7602–7625.
Govorov, A.O., Bryant, G.W., Zhang, W., Skeini, T., Lee, J., Kotov, N.A., Slocik, J.M., Naik, R.R., 2006. Nano Lett. 6, 984–994.
Grandjean, V., Yaman, R., Cuzin, F., Rassoulzadegan, M., 2007. PLoS ONE 2, e1136.
Hatada, I., Hayashizaki, Y., Hirotsune, S., Komatsubara, H., Mukai, T., 1991. Proc. Natl. Acad. Sci. 88, 9523–9527.
Heithoff, D.M., Sinsheimer, R.L., Low, D.A., Mahan, M.J., 1999. Science 284, 967–970.
Hu, J., Zhang, C., 2011. Biosens. Bioelectron. 31, 451–457.
Jiang, C., Yan, C.Y., Huang, C., Jiang, J.H., Yu, R.Q., 2012. Anal. Biochem. 423, 224–228.
Jiang, H., Ju, H.X., 2007. Anal. Chem. 79, 6690–6696.
Kass, S.U., Landsberger, N., Wolffe, A.P., 1997. Curr. Biol. 7, 157–165.
Kang, Q., Chen, Y.F., Li, C.C., Cai, Q.Y., Yao, S.Z., Grimes, C.A., 2011. Chem. Commun. 47, 12509–12511.
Khan, N., Afaq, F., Syed, D.N., Mukhtar, H., 2008. Carcinogenesis 29, 1049–1056.
Kuang, D.B., Ito, S., Wenger, B., Klein, C., Moser, J.E., Humphry-Baker, R., Zakeeruddin, S.M., Gratzel, M., 2006. J. Am. Chem. Soc. 128, 4146–4154.
Kurita, R., Arai, K., Nakamoto, K., Niwa, D.O., 2012. Anal. Chem. 84, 1799–1803.
Lee, J., Hernandez, P., Lee, J., Govorov, A.O., Kotov, N.A., 2007. Nat. Mater. 6, 291–295.
Li, J., Yan, H., Wang, K., Tan, W., Zhou, X., 2007. Anal. Chem. 79, 1050–1056.
Li, Y., Huang, C.C., Zheng, J.B., Qi, H.L., 2012. Biosens. Bioelectron. 38, 407–410.
Li, Y., Luo, X.E., Yan, Z., Zheng, J.B., Qi, H.L., 2013. Chem. Commun. 49, 3869–3871.
Liu, S.N., Wu, P., Li, W., Zhang, H., Cai, C.X., 2011. Chem. Commun. 47, 2844–2846.
Liu, T., Zhao, J., Zhang, D., Li, G., 2009. Anal. Chem. 82, 229–233.
Low, D.A., Weyand, N.J., Mahan, M.J., 2001. Infect. Immun. 69, 7197–7204.
Lu, H.Y., Hu, N.F., 2006. Electroanalysis 18, 1511–1522.
Lyko, F., Ramsahoye, B.H., Jaenisch, R., 2000. Nature 408, 538–540.
McLaughlin, L.W., Benseler, F., Graeser, E., Piel, N., Scholtissek, S., 1987. Biochemistry 26, 7238–7245.
Miyamoto, K., Fukutomi, T., Akashi-Tanaka, S., Hasegawa, T., Asahara, T., Sugimura, T., Ushijima, T., 2005. Int. J. Cancer. 116, 407–414.
Park, N.G., Lagemaat, J., Frank, A.J., 2000. J. Phys. Chem. B. 104, 8989–8994.
Reik, W., Dean, W., Walter, J., 2001. Science 293, 1089–1093.
Santz, P.A., Kamat, P.V., 2002. Phys. Chem. Chem. Phys. 4, 198–203.
Shan, Y., Xu, J.J., Chen, H.Y., 2009. Chem. Commun. 45, 905–907.
Song, G., Chen, C., Ren, J., Qu, X., 2009. ACS Nano 3, 1183–1189.
Tambwekar, S.V., Venugopal, D., Subrahmanyam, M., 1999. Int. J. Hydrog. Energy 24, 957–963.
Tsutsui, M., Matsubara, K., Ohshiro, T., Furuhashi, M., Taniguchi, M., Kawai, T., 2011. J. Am. Chem. Soc. 133, 9124–9128.
Vogel, R., Hoyer, P., Weller, H., 1994. J. Phys. Chem. 98, 3183–3188.
Wang, G.L., Yu, P.P., Xu, J.J., Chen, H.Y., 2009a. J. Phys. Chem. C. 113, 11142–11148.
Wang, G.L., Xu, J.J., Chen, H.Y., 2010. Nanoscale 2, 1112–1114.
Wang, G.L., Zhou, L.Y., Luo, H.Q., Li, N.B., 2013. Anal. Chim. Acta 768, 76–81.
Wang, J., Shan, Y., Zhao, W.W., Xu, J.J., Chen, H.Y., 2011. Anal. Chem. 83, 4004–4011.
Wang, M.J., Wang, L.Y., Yuan, H., Ji, X.H., Sun, C.Y., Ma, L., Bai, Y.B., Li, T.J., Li, J.H., 2004. Electroanalysis 16, 757–764.
Wang, X., Song, Y., Song, M., Wang, Z., Li, T., Wang, H., 2009b. Anal. Chem. 81, 7885–7891.
Wu, Z., Wu, Z.K., Tang, H., Tang, L.J., Jiang, J.H., 2013. Anal. Chem. 85, 4376–4383.
Yildiz, H.B., Freeman, R., Gill, R., Willner, I., 2008. Anal. Chem. 80, 2811–2816.
Yin, H.S., Zhou, Y.L., Xu, Z.N., Chen, L.J., Zhang, D., Ai, S.Y., 2013. Biosens. Bioelectron. 41, 492–497.
Zhang, H., Li, M.X., Fan, M.X., Gu, J.X., Wu, P., Cai, C.X., 2014. Chem. Commun. 50, 2932–2934.
Zhang, J., Song, S.P., Wang, L.H., Pan, D., Fan, C.H., 2007. Nat Protoc. 2, 2888–2895.
Zhang, X.R., Zhao, Y.Q., Li, S.G., Zhang, S.S., 2010. Chem. Commun. 46, 9173–9175.
Zhao, C., Qu, K.G., Song, Y.J., Ren, J.S., Qu, X.G., 2011a. Adv. Funct. Mater. 21, 583–590.
Zhao, W.W., Yu, P.P., Shan, Y., Wang, J., Xu, J.J., Chen, H.Y., 2012a. Anal. Chem. 84, 5892–5897.
Zhao, W.W., Wang, J., Xu, J.J., Chen, H.Y., 2011b. Chem. Commun. 47, 10990–10992.
Zhao, X.M., Zhou, S.W., Jiang, L.P., Hou, W.H., Shen, Q.M., Zhu, J.J., 2012b. Chem. Eur. J 18, 4974–4981.
Zhao, Y.X., Chen, F., Wu, Y.Y., Dong, Y.H., Fan, C.H., 2013. Biosens. Bioelectron. 42, 56–61.
Zhou, Y.L., Xu, Z.N., Wang, M., Sun, B., Yin, H.S., Ai, S.Y., 2014. Biosens. Bioelectron. 53, 263–267.
Zhu, W., An, Y.R., Luo, X.M., Wang, F., Zheng, J.H., Tang, L.L., Wang, Q.J., Zhang, Z.H., Zhang, W., Jin, L.T., 2009. Chem. Commun. 45, 2682–2684.